



Femtosecond studies of hydrated electron recombination following multiphoton ionization at 390 nm

J.L. McGowen^a, H.M. Ajo^a, J.Z. Zhang^{a,*}, Benjamin J. Schwartz^b

^a Department of Chemistry and Biochemistry, University of California, Santa Cruz, CA 95064, USA

^b Department of Chemistry and Biochemistry, University of Texas at Austin, Austin, TX 78712, USA

Received 26 May 1994; in final form 13 September 1994

Abstract

We report a femtosecond laser study of the power and wavelength dependence of the dynamics of the solvated electron produced through multiphoton ionization of water at 390 nm. While the localization dynamics are found to be in good agreement with previous studies exciting at 310 nm, nearly complete lack of geminate recombination is discovered on the time scale of up to 700 ps, in marked contrast to the substantial geminate recombination observed with 310 or 248 nm excitation. The results suggest that the electron–cation geminate recombination process is sensitive to the excitation wavelength both mechanistically and energetically.

1. Introduction

Solvated electrons play an important role in many chemical reactions in solution and have recently received a great deal of attention. The dynamics of hydrated electrons have been studied experimentally using ultrafast laser techniques [1–11] as well as theoretically using computer simulation methods [12–21]. Following photoejection from neat liquid water, the formation of hydrated electrons proceeds by a step-wise mechanism [1–3,12–14]. First, ejected electrons become localized in an electron excited state characterized by a transient absorption in the infrared in 110–180 fs. The equilibrium absorption spectrum of the hydrated electron subsequently appears in 240–540 fs as the localized excited electron undergoes internal conversion to the ground state. Computer simulations of the electron solvation process [12,13,17–19] have furthered the understand-

ing of the relaxation dynamics and equilibrium structure of pre-solvated, excited state and equilibrium hydrated electrons, and have led to the proposal of a detailed kinetic mechanism for electron localization following photoejection [14].

One of the most important issues surrounding the dynamics of hydrated electrons is electron–cation recombination [4–8,20,21]. After electrons are photoejected from water, they can diffuse and recombine with the nearby parent cationic species. Femtosecond studies performed with 310 nm multiphoton excitation (4 eV/photon) have found a significant amount (around 55%) of geminate recombination on the time scale of 100–150 ps [4–7], and the recombination rate was found to decrease at higher pump powers [4]. This power dependence has been explained by a model that includes two electron production channels, one involving a two-photon process (requiring at least 6.5 eV of energy) and the second involving a three-photon process (requiring at least 8.5 eV of energy) that dominates at higher

* Corresponding author.

pump power [4]. These two processes could not, however, be independently evaluated because the excitation wavelength (310 nm) used in these studies did not allow exclusion of either possible mechanism. Substantial recombination has also been observed in experiments using 620 nm multiphoton excitation [9]. A recent study by Sander et al. [8] using 248 nm multiphoton excitation (5 eV/photon) found less overall recombination (around 30%) as well as a slower recombination rate following two-photon ionization compared to the 310 nm experiments. These observations can still be explained on the basis of the greater excess energy available at 248 nm than at 310 nm, but suggest the possibility that the decay due to geminate recombination may be sensitive both to the excess energy available and the ionization channel through which the electrons are created.

In this Letter, we report a study of recombination of hydrated electrons in water created with multiphoton ionization at 390 nm. This wavelength has low enough energy (3.2 eV per photon) to exclude the two-photon process for the production of electrons that requires 6.5 eV of energy. A three-photon process would provide 9.6 eV of energy, which is between the 8 eV used in Refs. [1–7] and 10 eV used in Ref. [8]. Through this study, we hope to provide an independent evaluation of the electron–cation recombination mechanism. *The results we obtained at 390 nm show essentially no recombination up to 700 ps, independent of the pump power and probe wavelength.* This observation is an interesting contrast to those observed previously at 310, 620 and 248 nm and provides complementary information to the understanding of electron solvation and recombination.

2. Experimental

The experiments were performed using a pump–probe scheme with a regeneratively amplified, mode-locked femtosecond Ti–sapphire laser [22]. Pulses of 40 fs duration with 5 nJ/pulse energy at a repetition rate of 100 MHz were obtained from a home-built, mode-locked Ti–sapphire oscillator and amplified in a 1 kHz Ti–sapphire regenerative amplifier using chirped pulse amplification. The final output pulses, typically 150 fs with a pulse energy of 350 μ J centered at 780 nm, were doubled in a KDP crystal

to generate 30 μ J pulses of 390 nm light, which was attenuated to the desired level between 8 and 24 μ J/pulse using neutral density filters and used as the pump beam. Levels below 8 μ J/pulse produced a signal that was too small to be detected because of the non-linear dependence of the signal on the pump power (the signal size varied with pump intensity to the power of approximately 2.5), and levels above 24 μ J/pulse were found to give anomalous results due to white light generation in the flow jet and/or boiling in the static cuvette because of the 1 kHz repetition rate of the laser. The remaining fundamental light was focused into quartz to generate a white light continuum, from which the desired probe wavelength was selected using an interference band pass filter (\approx 10 nm fwhm). The pump and probe beams were focused with a 10 cm focal length lens and overlapped in a flow jet with a thickness of 100 μ m. Experiments performed in a 1 cm path length quartz cuvette produced identical results with a larger signal size but slightly poorer time resolution due to the longer path length. Doubly distilled water was used in the experiments; measurements using HPLC grade water (Fisher) produced identical results.

3. Results and discussion

3.1. Localization dynamics

Since the excited state of the hydrated electron absorbs significantly to the red of the equilibrium ground state electron, formation of the excited state followed by internal conversion produces a distinct transient spectral signature. At wavelengths to the red of \approx 800 nm where the excited state absorption cross section is larger, absorption transients should show an initial rise due to formation of excited state electrons, followed by an absorption decay as the radiationless transition produces the ground state equilibrium electron with its lower oscillator strength. To the blue of \approx 800 nm, absorption transients should display an overall appearance time due to the formation of excited state electrons followed by the increase in cross section accompanying the non-adiabatic relaxation to the ground state. Fig. 1 shows the initial time evolution of the hydrated electron absorption produced following multiphoton electron ejection at 390

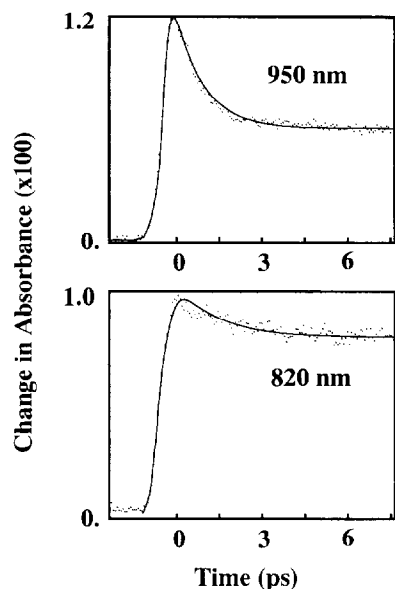


Fig. 1. Electron solvation dynamics at two different probe wavelengths, 820 and 950 nm following multiphoton ionization of water at 390 nm. The dotted curves are experimental data and the solid curves are fits using a function consisting of a single exponential rise with a time constant of 150 fs and an exponential decay with a time constant of 500 fs, plus an offset, convoluted with a Gaussian of 200 fs (fwhm) representing the instrument function.

nm probed at both 820 and 950 nm. The transient spectra for both wavelengths feature a very fast rise followed by a fast decay and then an essentially flat offset. These curves are fit by a single exponential rise with a time constant of 150 ± 50 fs, and an exponential decay with a time constant of 500 ± 150 fs, plus an offset (or very slow decay with a time constant greater than 7 ns), convoluted with a Gaussian of 200 fs (fwhm) representing the instrument function (cross-correlation of the pump and probe pulses). The fast rise and fast decay are attributed to the formation of the presolvated (excited state) and solvated (ground state) electrons, respectively, and thus indicate that the presolvated electron is formed within the laser pulse (≈ 150 fs) while the internal conversion takes place with a time constant of ≈ 500 fs. These assignments are consistent with additional transients taken at 660 and 780 nm which show appearance times comparable to the instrumental resolution (a few hundred femtoseconds). All these results are in excellent agreement with previous

experimental observations [1–3] and computer simulation studies [12–14], and serve to provide a consistent picture of the electron localization process.

3.2. Recombination dynamics

Once the localization process is complete, further decay of the transient absorption is due to loss of the absorbing ground state electrons through geminate recombination. The spectral signature for this process is an identical decay at every wavelength reflecting the simple loss of overall population. Fig. 2 shows representative data taken with probe wavelengths of 950, 820, 780 and 660 nm on the hundreds of picoseconds time scale for two different pump intensities. The fast rise and decay dynamics due to electron localization prominent in Fig. 1 are complete within

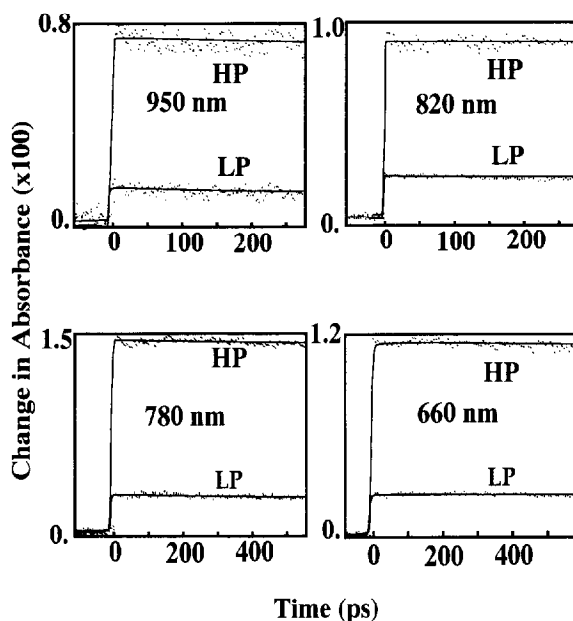


Fig. 2. Pump power dependence of the dynamics probed at different wavelengths as shown in the figure. The high power (HP) is 20 $\mu\text{J}/\text{pulse}$ for the 390 nm pump pulse and the low power (LP) is 10 $\mu\text{J}/\text{pulse}$. The dotted curves are experimental data and the solid lines are fits using the expression based on a one-dimensional random walk model as used in Ref. [8]. $A(t) = A_0 \times [\alpha \operatorname{erf}(\tau_r/t)^{1/2} + 1 - \alpha]$. The best fits require α to be smaller than 0.05, which indicates an escape yield of less than 5%. Within the signal-to-noise, a reasonable fit can be obtained for values of τ_r larger than 10 ps. Since there is essentially no decay, the exact value of τ_r is of little consequence in the fits.

the first few data points and hence are not readily evident in these longer time scans. Our longest time scan is limited to about 700 ps by the length of the translation stage, but if we assume the seemingly flat offset actually decays on a longer time scale, we can fit this long time data using a single exponential decay that requires a time constant of at least 7 ns.

The most notable feature of the data is the essential lack of any decay on the hundreds of picoseconds time scale. This is quite an intriguing contrast to the decays attributed to electron–cation recombination observed when 310 nm (55% recombination) [4–7] and 248 nm (30% recombination) [8] were used as excitation wavelengths. Fits of our transients in Fig. 2 to a simple one-dimensional random walk model [8] find that the recombination yield for 390 nm excitation is $\leq 5\%$ (the optimal fit gives essentially zero recombination, but the signal-to-noise does not allow us to completely eliminate the possibility of up to 5% recombination on the 700 ps time scale). To verify that our absorption transients were indeed due to hydrated electrons, we performed additional experiments in the presence of an electron scavenger (0.12 M HCl). In these acidic solutions, we found the transients decayed much more quickly, losing $\approx 50\%$ of their amplitude over 600 ps. This decay is clearly the result of non-geminate electron–cation recombination with the scavenger hydronium ions, and confirms that the signal is in fact due to the electron.

Comparison of the results at different powers also indicates that the recombination dynamics are essentially independent of the pump power at all the probe wavelengths investigated. Fig. 2 also compares the results at pump powers of 10 (labeled LP in the figure) and 20 (labeled HP in the figure) $\mu\text{J}/\text{pulse}$, corresponding to power densities of about 18 and 36 GW/cm^2 , respectively. Measurements carried out at other powers over the range between 8 and 24 $\mu\text{J}/\text{pulse}$ showed identical transient spectral features. While a greater range of intensities is clearly desirable, the experimental difficulties outlined in Section 2 provide the present limit of only a factor of ≈ 3 in pump power. However, previous work with a 310 nm pump wavelength found a readily observable intensity dependence to the electron geminate recombination when the pump power was varied over a factor of only 2.5 [4]. Thus, in addition to finding virtually no recombination, the 390 nm data pre-

sented here provides another contrast to previous work at other pump wavelengths: the lack of an intensity dependence to the geminate recombination with a factor of 3 variance in the pump power. The most likely explanation for these observed contrasts is that the recombination process is sensitive not only to the amount of excess energy available to the solvated electron (energetic) but also the pathway through which the solvated electron is produced (mechanistic).

3.3. Mechanisms of electron production

One of the most basic questions surrounding the issue of electron–cation geminate recombination is how electrons are produced from multiphoton excitation of neat liquid water. Since the threshold for direct photoionization of liquid water is unknown and there are many possible autoionization or solvent-assisted mechanisms for electron ejection from highly excited water, it is of little surprise that this question has been the subject for a great deal of speculation [4–8,23–25]. In Ref. [23], Sander et al. present an excellent summary of the possible competing channels for producing electrons in water at different excitation energies. In Fig. 3, a schematic energy diagram is shown, illustrating the different photon energies used in the three (310, 248 and 390 nm) femtosecond experiments superimposed on the available ionization thresholds [23]. Starting at

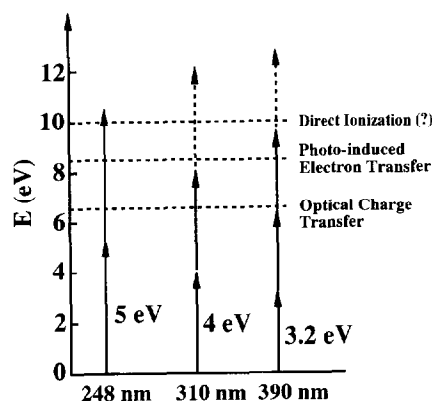


Fig. 3. Schematic illustration of the various ionization thresholds of liquid water and the different photon energies used in the three femtosecond experiments (248, 310 and 390 nm). Much of this information is adapted from Fig. 2 of Ref. [23].

energies above 6.5 eV, an optical charge transfer (OCT) mechanism is the primary means of electron production. At energies around 8.5 eV, photoinduced electron transfer (PIET) [24] begins to successfully compete as a means of electron production. Direct photoionization into the conduction band is not expected to play an important role at energies below 10 eV.

The ideas underlying Fig. 3 are able to successfully explain the results of the 310 and 248 nm electron ejection experiments. In the 310 nm experiment, the observed recombination decay can be attributed to electrons generated via a two-photon process (8 eV available energy from two 4 eV photons) through the OCT mechanism which becomes accessible at 6.5 eV. In the 248 nm experiment, two-photon excitation (10 eV available energy from two 5 eV photons) provides access to both the OCT and PIET pathways. In this case, the excess energy for electrons produced by the OCT mechanism is larger than for 310 nm excitation, with ≈ 3.5 eV energy available from 248 nm excitation but only ≈ 1.5 eV from 310 nm excitation. This greater excess energy (in possible combination with the additional presence of the PIET mechanism) leads to production of electrons with larger thermalization distances for 248 than 310 nm excitation, and thus explains the lower recombination yield and rate observed in the 248 nm experiment. The intensity dependence observed in the 310 nm experiments, i.e. the smaller recombination amplitudes at higher pump powers, can also be explained by a similar argument. At higher pump powers, the production of electrons via three-photon ionization (12 eV available energy) becomes more important, leading to generation of electrons by either the OCT or PIET (or possibly even direct ionization) mechanisms with larger thermalization distances and hence the observed lower recombination amplitude [4].

In the present study using 390 nm excitation, two-photon excitation (6.4 eV available energy from two 3.2 eV photons) is not enough to access any of the proposed ionization channels. Even *if* the 6.5 eV threshold for OCT is actually smaller than 6.4 eV and the two-photon transition becomes attainable, extremely little excess energy would be expected. This would result in very fast recombination due to the small thermalization distance, and the resulting spectral signature would likely be lost under the absorp-

tion changes due to localization dynamics. Thus, the most likely process for the generation of persistent solvated electrons at 390 nm is via three-photon excitation (9.6 eV available energy). This provides enough energy to activate both the OCT and PIET ionization mechanisms, leaving ≈ 3.1 eV excess energy for the OCT channel. This excess energy is lower than the excess energies available in either the (three-photon) 310 nm or the (two-photon) 248 nm experiments. To explain our observation of essentially no recombination decay up to 700 ps in the schematic of Fig. 3, we would need a much larger excess energy *if* the decay were determined completely by the energetics of the solvated electron. A four-photon transition would provide this excess energy but is not very likely given the intensities used (18–36 GW/cm²), especially considering that the power densities used in the present experiment were similar or somewhat lower than those used in the 310 nm experiments [1–7]. Therefore, energetic arguments alone do not seem to be able to explain the lack of geminate recombination observed with 390 nm excitation.

We propose that the explanation for the lack of electron-cation recombination lies in the production mechanism for the hydrated electron. Since the 9.6 eV energy used in the current 390 nm experiment (assuming a three-photon process) is in between 8 and 10 eV, a smooth transition between the OCT and PIET mechanisms would not be expected to produce the significant change in the recombination dynamics observed. It is conceivable that electron production, and hence, recombination is not only dependent on the excitation wavelength through the excess energy, but is also wavelength sensitive due the specific pathway through which the electron is generated. Thus, there may be an additional ionization pathway causing the different recombination dynamics observed with 390 nm excitation. Since the selection rules for two-photon excitation (310 and 248 nm) are completely different from three-photon excitation (390 nm), the symmetries of the molecular states involved in the optical excitation may be important in the overall process of electron production. In the gas phase, the first absorption maximum of water near 7.5 eV is assigned to a transition to the R3s molecular Rydberg state [23]. This transition is blue-shifted to ≈ 8.2 eV in liquid water due to confinement of the extended molecular Rydberg orbital

[26]. Thus, the absorption around 8.0 eV is attributed to an OCT band superimposed on the broadened and weakened R3s absorption. At 10 eV there is an absorption maximum in the VUV spectrum of water due to the transitions that terminate in the R3p states which arise from gas phase transitions with rotational and vibrational structure [23,27]. Since the coupling of these underlying transitions to various electron production mechanisms may be quite different, excitation into a particular state may dramatically change the electron production mechanism. Therefore, the observed recombination dynamics can be quite sensitive to excitation wavelength because different final electronic states may be accessed by different excitation energies or selection rules.

It is clear that a definitive explanation for all the observations is not possible at this point, however, the apparent lack of electron–cation geminate recombination at 390 nm and its implication of a mechanistic dependence on excitation wavelength is significant to the understanding of the behavior of solvated electrons in water. Further investigation is necessary to clarify the issues involved. A tunable femtosecond pump source should be useful to fully characterize the wavelength dependence of the dynamics of the solvated electron in water and to help bridge the gap between experiments performed up to this point.

4. Conclusions

We have carried out femtosecond studies of solvated electrons in water produced through a presumably three-photon ionization process using 390 nm excitation. We have shown that there is no noticeable geminate recombination on the time scale of up to 700 ps, in contrast to previous studies exciting at 310 and 248 nm. This study suggests that the dynamics of electron–cation geminate recombination may be sensitive to the pump wavelength through both the excess energy and the selection rules of the electron production mechanism.

Acknowledgement

The authors wish to thank Professor F.H. Long, Professor I. Benjamin, Professor K.B. Eisenthal, Pro-

fessor P.J. Rossky and Professor J.-P. Jay-Gerin for fruitful discussions. This work was supported in part by a Faculty Research grant from the University of California at Santa Cruz and by a grant from the Petroleum Research Fund administered by the American Chemical Society. BJS gratefully acknowledges the support of an NSF post-doctoral fellowship in chemistry.

References

- [1] A. Migus, Y. Gauduel, J.-L. Martin and A. Antonetti, *Phys. Rev. Letters* 58 (1987) 1559.
- [2] S. Pommeret, A. Antonetti and Y. Gauduel, *J. Am. Chem. Soc.* 113 (1991) 9105.
- [3] F.H. Long, H. Lu and K.B. Eisenthal, *Phys. Rev. Letters* 64 (1990) 1469.
- [4] F.H. Long, H. Lu, X. Shi and K.B. Eisenthal, *Chem. Phys. Letters* 185 (1991) 47.
- [5] F.H. Long, H. Lu and K.B. Eisenthal, *Chem. Phys. Letters* 160 (1989) 464.
- [6] H. Lu, F.H. Long, R.M. Bowman and K.B. Eisenthal, *J. Phys. Chem.* 93 (1989) 27.
- [7] Y. Gauduel, S. Pommeret, A. Migus and A. Antonetti, *Chem. Phys. Letters* 149 (1990) 1.
- [8] M.U. Sander, K. Luther and J. Troe, *J. Phys. Chem.* 97 (1993) 11489.
- [9] C. Pepin, D. Houde, H. Remita, T. Goulet and J.-P. Jay-Gerin, *Phys. Rev. Letters* 69 (1992) 3389.
- [10] Y. Kimura, J.C. Alfano, P.K. Walhout and P.F. Barbara, *J. Phys. Chem.* 98 (1994) 3450.
- [11] J.C. Alfano, P.K. Walhout, Y. Kimura and P.F. Barbara, *J. Chem. Phys.* 98 (1993) 5996.
- [12] T. Murphrey and P.J. Rossky, *J. Chem. Phys.* 99 (1993) 515.
- [13] F. Webster, J. Schnitker, M. Freidrichs, R. Freisner and P.J. Rossky, *Phys. Rev. Letters* 66 (1991) 3172.
- [14] E. Keszei, S. Nagy, T.H. Murphrey and P.J. Rossky, *J. Chem. Phys.* 99 (1993) 2004.
- [15] A. Wallqvist, G. Martyna and B.J. Berne, *J. Phys. Chem.* 92 (1988) 1721.
- [16] R.N. Barnett, U. Landman and A. Nitzan, *J. Chem. Phys.* 93 (1990) 8187.
- [17] B.J. Schwartz and P.J. Rossky, *J. Chem. Phys.*, in press.
- [18] B.J. Schwartz and P.J. Rossky, *J. Phys. Chem.* 98 (1994) 4489.
- [19] B.J. Schwartz and P.J. Rossky, *Phys. Rev. Letters* 72 (1994) 3282.
- [20] T. Goulet and J.P. Jay-Gerin, *J. Phys. Chem.* 93 (1989) 7532.
- [21] T. Goulet and J.P. Jay-Gerin, *J. Chem. Phys.* 96 (1991) 5076.
- [22] J.Z. Zhang, R.H. O'Neil and T.W. Roberti, *J. Phys. Chem.* 98 (1994) 3859.

- [23] M.U. Sander, K. Luther and J. Troe, *Ber. Bunsenges. Physik. Chem.* 97 (1993) 953, and references therein.
- [24] E. Keszei and J.-P. Jay-Gerin, *Can. J. Chem.* 70 (1992) 21.
- [25] A. Bernas and D. Grand, *J. Phys. Chem.* 98 (1994) 3440.
- [26] P. Han and D.M. Bartels, *J. Phys. Chem.* 94 (1990) 5824.
- [27] W.A. Goddard III and W.J. Hunt, *Chem. Phys. Letters* 24 (1974) 464.